Oxygen Storage Hot Paper

DOI: 10.1002/ange.201408464

Metal–Organic Frameworks for Oxygen Storage**

Jared B. DeCoste, Mitchell H. Weston, Patrick E. Fuller, Trenton M. Tovar, Gregory W. Peterson, M. Douglas LeVan,* and Omar K. Farha**

Abstract: *We present a systematic study of metal–organic frameworks (MOFs) for the storage of oxygen. The study starts with grand canonical Monte Carlo simulations on a suite of 10000 MOFs for the adsorption of oxygen. From these data, the MOFs were down selected to the prime candidates of HKUST-1 (Cu-BTC) and NU-125, both with coordinatively unsaturated Cu sites. Oxygen isotherms up to 30 bar were measured at multiple temperatures to determine the isosteric heat of adsorption for oxygen on each MOF by fitting to a Toth isotherm model. High pressure (up to 140 bar) oxygen isotherms were measured for HKUST-1 and NU-125 to determine the working capacity of each MOF. Compared to the zeolite NaX and Norit activated carbon, NU-125 has an increased excess capacity for oxygen of 237% and 98%, respectively. These materials could ultimately prove useful for oxygen storage in medical, military, and aerospace applications.*

Metal–organic frameworks (MOFs) have been of broad interest for their wide variety of applications such as gas storage,[1] separations,[2] sensing,[3] catalysis,[4] light harvesting,[5] and toxic gas removal.[6] However, to date there has been minimal focus on oxygen storage. The storage of oxygen has applications for use by first responders and military personnel, as well as in the medical and aerospace industries. In these applications there is a need to increase the amount of oxygen stored per unit volume, or reduce the oxygen storage pressure due to safety concerns. Porous carbons such as MSC-7R and AX-21,[7] as well as the zeolite NaX,[8] have been tested for oxygen storage. The biggest drawback of activated carbons is the heterogeneity of the pore sizes which makes their design difficult. However, the ability to tune the pore geometry and size of MOFs makes them excellent candidates for oxygen storage applications.[9]

Prior to performing experiments, 10000 hypothetical MOF materials were simulated for oxygen capacities to down select which MOFs were studied experimentally. The database was created through the use of established high-speed MOF generation techniques[10] and designed to maximize the breadth of material properties over a minimal set of frameworks. Each material in the database was then run through a charging algorithm and a grand canonical Monte Carlo (GCMC) simulation, returning calculated room temperature oxygen adsorption quantities as a function of pressure, as depicted in Figure 1.[1f,11] The most promising materials from this study were then curated, producing a final

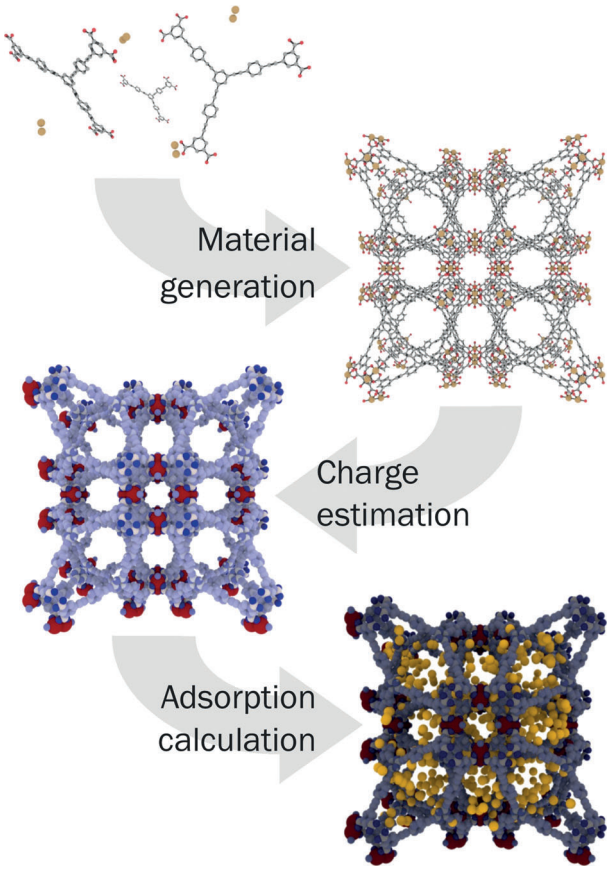

Figure 1. Generation of MOFs and their computational screening for sorption characteristics.

[*] Dr. J. B. DeCoste
Leidos, Inc.
PO Box 68, Gunpowder, MD 21010 (USA)
E-mail: jared.b.decoste2.ctr@mail.mil
Dr. M. H. Weston, P. E. Fuller, Dr. O. K. Farha
NuMat Technologies
8025 Lamon Avenue, Skokie, IL 60077 (USA)
Dr. O. K. Farha
Department of Chemistry, Northwestern University
2145 Sheridan Rd., Evanston, IL 60208 (USA)
E-mail: o-farha@northwestern.edu
T. M. Tovar, Dr. M. D. LeVan
Department of Chemical and Biomolecular Engineering
Vanderbilt University
PMB 351604, Nashville, TN 37235 (USA)
E-mail: m.douglas.levan@vanderbilt.edu
G. W. Peterson
Edgewood Chemical Biological Center
5183 Blackhawk Rd., Aberdeen Proving Ground, MD 21010 (USA)

[**] J.B.D. and G.W.P. gratefully acknowledge the Defense Threat Reduction Agency (DTRA) for financial support under BA07PRO104, and M.D.L. acknowledges DTRA under W911SR-13-C-0014.

Supporting information for this article is available on the WWW under http://dx.doi.org/10.1002/anie.201408464.

list of materials for experimental validation. From the information obtained in these simulations, it was determined that HKUST-1[12] (Figure S1) and NU-125[13] (Figure S2) were prime candidates for further studies, based on their superior ability to adsorb oxygen and currently known synthesis techniques. These MOFs, along with UiO-66 (Figure S3), a zirconium based MOF known for its exceptional stability,[9a,14] an activated carbon (Norit SX ultra, herein referred to as N-AC), and zeolite NaX were examined by measuring oxygen isotherms up to 30 bar at multiple temperatures and high-pressure oxygen isotherms up to 140 bar at room temperature. The 30 bar metric was chosen due to safety concerns with higher pressure oxygen at elevated temperatures (up to 348 K), whereas the 140 bar metric at ambient temperature was chosen based on the standard pressure used in medical oxygen tanks. N-AC was used as a baseline sorbent, as previous works have shown that activated carbons can provide high oxygen storage capacities.[7]

Excess oxygen isotherms for HKUST-1, NU-125, and UiO-66 were measured for pressures up to approximately 30 bar at 298 K and are compared to N-AC and NaX in Figure 2. At pressures less than 2 bar, the inset shows that

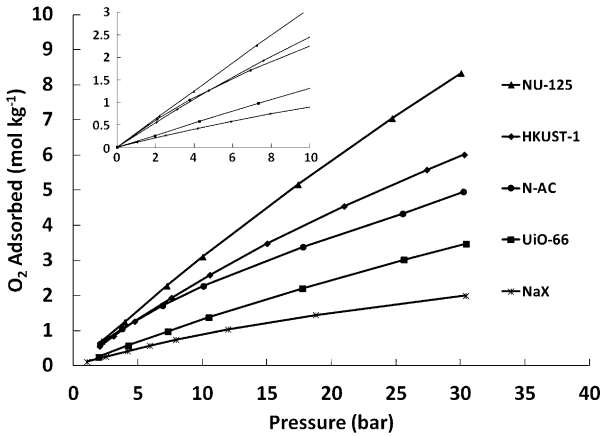

Figure 2. Excess oxygen isotherms measured at 298 K up to 30 bar.

NU-125 and N-AC have similar O_2 capacities, whereas HKUST-1 has a slightly lower capacity. The isotherm for N-AC curves downward, while the HKUST-1 and NU-125 isotherms remain much more linear. At 30 bar NU-125, HKUST-1, and N-AC have excess O_2 capacities of 8.3, 6.0, and 5.0 mol kg^{-1}, respectively. In contrast, UiO-66 and NaX have significantly lower capacities of 3.5 and 2.0 mol kg^{-1}, respectively. Ideal materials exhibit oxygen isotherms characterized by gradual slopes at low pressures, indicating minimal sorbent–sorbate interactions at low pressures, and high overall capacities at high pressures, thereby maximizing working deliverable capacity.

Excess oxygen isotherms were measured at 298, 323, and 348 K for each MOF and N-AC (Figures S4–S7). From this data and the oxygen isotherms of NaX reported elsewhere,[8] the isosteric heat of adsorption of oxygen was calculated for each material at 298 K using the Toth model (Table S1, Figure S8). The Toth equation can be used to describe the temperature and pressure dependence of adsorption over wide ranges and is described in detail in the Supporting Information.[15] At high pressures, adsorption is not likely to form a monolayer as assumed by a Langmuir model, and the Toth equation allows an extra empirical parameter for fitting. This work focuses on the adsorption of oxygen at high pressures; therefore, data were not obtained below 1 bar, where high-energy sorbent–sorbate interactions occur. It was observed that the isosteric heat of adsorption for N-AC decreases as a function of increased loading at 298 K, indicative of adsorption with a heterogeneous material. On the other hand, HKUST-1, NU-125, and NaX each show a relatively stable isosteric heat of adsorption with increased loading at 298 K, indicative of adsorption dominated mainly by geometric phenomena on a more homogeneous surface. It is important to have a high capacity while minimizing the strong interactions of the material with the adsorbate, because these interactions typically dominate at pressures below the working pressure of gas cylinders. Both HKUST-1 and NU-125 contain coordinatively unsaturated copper sites; however, these sites do not seem to preferentially adsorb oxygen at the high pressures studied here. The adsorption of oxygen was observed to be geometric in the GCMC calculations and oxygen did not cluster at the Cu sites. However, it has been shown that coordinatively unsaturated metal sites can enhance the adsorption of oxygen at low pressures.[16] Furthermore, the isosteric heat of adsorption for HKUST-1 is higher than that for NU-125, likely due to the smaller pore size and a higher concentration of Cu sites in HKUST-1.

Based on the isotherms studied up to 30 bar, we decided to investigate HKUST-1, NU-125, and N-AC further. These materials were studied up to pressures of 140 bar at room temperature and compared to NaX from Wang et al.,[8] with the excess oxygen isotherms shown in Figure 3 and Table 1. The isotherm for each material compares well to the predicted outcome from the Toth model and the oxygen isotherm predicted from the GCMC calculations (HKUST-1 and NU-125 only; Figures S9–S12). NU-125 and HKUST-1 have excess capacities of 98 and 75% greater than that of the N-AC at 140 bar, respectively. Based on volumetric

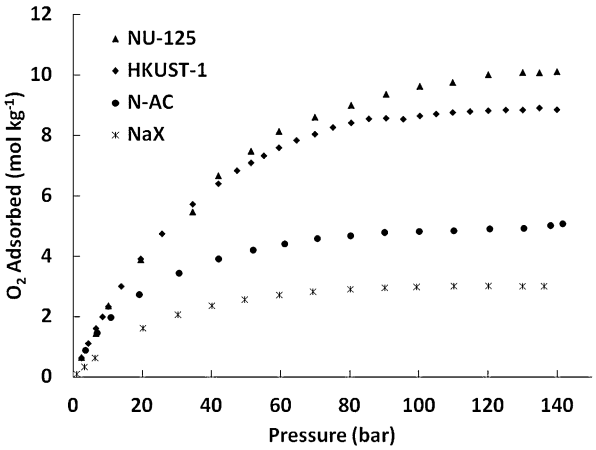

Figure 3. Excess oxygen adsorption isotherms measured at room temperature up to 140 bar.

Table 1: Surface area, pore volume, excess and absolute oxygen capacity, and deliverable oxygen capacity for NU-125, HKUST-1, activated carbon, and NaX.

Material	BET surface area [$m^2 g^{-1}$]	Pore volume [$cc g^{-1}$]	Excess O_2 adsorbed[b] [$mol kg^{-1}$]	Absolute O_2 adsorbed[b] [$mol kg^{-1}$]	Deliverable O_2[c] [$mol kg^{-1}$]
NU-125	2880	1.29	10.1	17.4	15.7
HKUST-1	1880	0.77	8.9	13.2	11.9
N-AC	1040	0.76	5.1	9.4	8.0
NaX[a]	560	0.27	3.0	7.2	6.6

[a] From Ref. [7]. [b] Capacity at 140 bar. [c] Absolute capacity at 140 bar minus the absolute capacity at 5 bar.

parameters, HKUST-1 and NU-125 have capacities of 114 and 89% greater than an empty oxygen cylinder at 140 bar, respectively.

For HKUST-1 and NU-125, adsorption and desorption cycles were performed to determine the structural integrity of the MOFs upon exposure to high pressure oxygen. It can be seen in Figure 4 that for each of the MOFs there is no appreciable loss in capacity over 50 cycles run up to 30 bar, and it can therefore be concluded that the structural integrity is maintained in the presence of oxygen at the pressures studied. This is an important feature when considering recharging cycles.

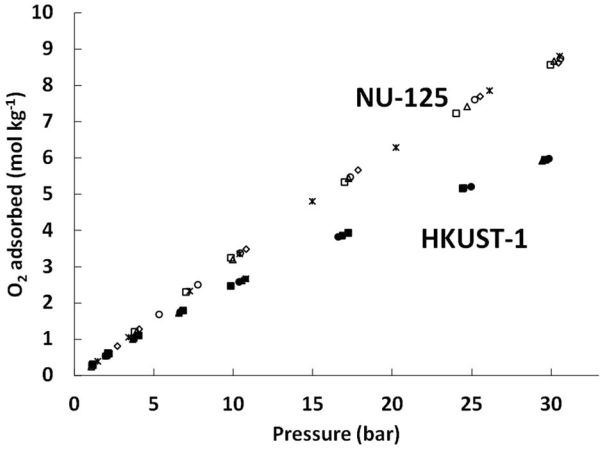

Figure 4. Excess oxygen adsorption isotherms measured at 1 (square), 5 (diamond), 10 (triangle), 20 (star), and 50 (circle) cycles at 298 K and pressures up to 30 bar for NU-125 (hollow symbols) and HKUST-1 (solid symbols).

The high capacities and ability to be cycled without a loss in capacity make HKUST-1 and NU-125 ideal potential adsorbents for oxygen storage. These MOFs are comparable to the current state of the art carbons and outperform zeolites for oxygen storage. A substantial increase in capacity allows for a cylinder at high pressure to store much more oxygen, therefore requiring less frequent recharging, ultimately reducing the cost of oxygen storage, or even allowing for smaller cylinders for easier transport. HKUST-1 and NU-125 show an increase in capacity at 140 bar of approximately 114 and 89%, respectively, over an empty cylinder. These MOFs could also allow for one to obtain a similar capacity to an empty cylinder at a decreased pressure, which could allow for the use of less heavy-duty cylinder components, ultimately reducing the cost and total mass of the oxygen storage device. Increased capacities in oxygen cylinders can lead to longer dives for divers, more efficient storage for fighter pilots and astronauts, and a better quality of life for those who are dependent on medical oxygen.

Experimental Section

The procedures for synthesizing HKUST-1, NU-125,[13] and UiO-66[17] are outlined in detail in the Supporting Information. The activated carbon Norit SX ultra (Aldrich, 53663) was purchased and used without further modification.

A volumetric apparatus was used to collect oxygen isotherms at 298, 313, and 348 K over the range of 1–30 bar, as described in detail in the Supporting Information and elsewhere.[8] This apparatus was also used to collect oxygen isotherms at 298 K after repeated adsorption/desorption cycles. High pressure oxygen isotherms (up to 140 bar) were measured using a Micromeritics HPVA II-200 Volumetric Sorption Analyzer.

Received: August 22, 2014
Published online: October 15, 2014

Keywords: adsorption · metal–organic frameworks · microporous materials · oxygen

[1] a) S. S. Han, J. L. Mendoza-Cortes, W. A. Goddard III, *Chem. Soc. Rev.* **2009**, *38*, 1460 – 1476; b) K. Sumida, D. L. Rogow, J. A. Mason, T. M. McDonald, E. D. Bloch, Z. R. Herm, T.-H. Bae, J. R. Long, *Chem. Rev.* **2012**, *112*, 724 – 781; c) M. P. Suh, H. J. Park, T. K. Prasad, D.-W. Lim, *Chem. Rev.* **2012**, *112*, 782 – 835; d) R. B. Getman, Y.-S. Bae, C. E. Wilmer, R. Q. Snurr, *Chem. Rev.* **2012**, *112*, 703 – 723; e) H. Wu, Q. Gong, D. H. Olson, J. Li, *Chem. Rev.* **2012**, *112*, 836 – 868; f) T. Düren, Y.-S. Bae, R. Q. Snurr, *Chem. Soc. Rev.* **2009**, *38*, 1237 – 1247; g) J. Liu, P. K. Thallapally, B. P. McGrail, D. R. Brown, J. Liu, *Chem. Soc. Rev.* **2012**, *41*, 2308 – 2322.

[2] a) J.-R. Li, R. J. Kuppler, H.-C. Zhou, *Chem. Soc. Rev.* **2009**, *38*, 1477 – 1504; b) J.-R. Li, J. Sculley, H.-C. Zhou, *Chem. Rev.* **2012**, *112*, 869 – 932; c) Q. Yang, D. Liu, C. Zhong, J. R. Li, *Chem. Rev.* **2013**, *113*, 8261 – 8323.

[3] a) L. E. Kreno, K. Leong, O. K. Farha, M. Allendorf, R. P. Van Duyne, J. T. Hupp, *Chem. Rev.* **2012**, *112*, 1105 – 1125; b) Y. Cui, Y. Yue, G. Qian, B. Chen, *Chem. Rev.* **2012**, *112*, 1126 – 1162; c) J. Rocha, L. D. Carlos, F. A. A. Paz, D. Ananias, *Chem. Soc. Rev.* **2011**, *40*, 926 – 940.

[4] a) J. Lee, O. K. Farha, J. Roberts, K. A. Scheidt, S. T. Nguyen, J. T. Hupp, *Chem. Soc. Rev.* **2009**, *38*, 1450 – 1459; b) L. Ma, C. Abney, W. Lin, *Chem. Soc. Rev.* **2009**, *38*, 1248 – 1256.

[5] a) C. A. Kent, D. Liu, L. Ma, J. M. Papanikolas, T. J. Meyer, W. Lin, *J. Am. Chem. Soc.* **2011**, *133*, 12940 – 12943; b) S. Jin, H.-J. Son, O. K. Farha, G. P. Wiederrecht, J. T. Hupp, *J. Am. Chem. Soc.* **2013**, *135*, 955 – 958; c) H.-J. Son, S. Jin, S. Patwardhan, S. J. Wezenberg, N. C. Jeong, M. So, C. E. Wilmer, A. A. Sarjeant, G. C. Schatz, R. Q. Snurr, O. K. Farha, G. P. Wiederrecht, J. T. Hupp, *J. Am. Chem. Soc.* **2013**, *135*, 862 – 869; d) C. A. Kent, B. P. Mehl, L. Ma, J. M. Papanikolas, T. J. Meyer, W. Lin, *J. Am. Chem. Soc.* **2010**, *132*, 12767 – 12769.

[6] a) N. A. Khan, Z. Hasan, S. H. Jhung, *J. Hazard. Mater.* **2013**, *244 – 245*, 444 – 456; b) E. Barea, C. Montoro, J. A. R. Navarro,

Chem. Soc. Rev. **2014**, *43*, 5419 – 5430; c) J. B. DeCoste, G. W. Peterson, *Chem. Rev.* **2014**, *114*, 5695 – 5727.
[7] a) L. A. Mitchell, T. M. Tovar, M. D. LeVan, *Carbon* **2014**, *74*, 120 – 126; b) Y. Zhou, L. Wei, J. Yang, Y. Sun, L. Zhou, *J. Chem. Eng. Data* **2005**, *50*, 1068 – 1072; c) Y. S. Bae, C. H. Lee, *Carbon* **2005**, *43*, 95 – 107.
[8] Y. Wang, B. Helvensteijn, N. Nizamidin, A. M. Erion, L. A. Steiner, L. M. Mulloth, B. Luna, M. D. LeVan, *Langmuir* **2011**, *27*, 10648 – 10656.
[9] a) J. H. Cavka, S. Jakobsen, U. Olsbye, N. Guillou, C. Lamberti, S. Bordiga, K. P. Lillerud, *J. Am. Chem. Soc.* **2008**, *130*, 13850 – 13851; b) M. Kandiah, M. H. Nilsen, S. Usseglio, S. Jakobsen, U. Olsbye, M. Tilset, C. Larabi, E. A. Quadrelli, F. Bonino, K. P. Lillerud, *Chem. Mater.* **2010**, *22*, 6632 – 6640; c) M. Eddaoudi, J. Kim, N. Rosi, D. Vodak, J. Wachter, M. O'Keeffe, O. M. Yaghi, *Science* **2002**, *295*, 469 – 472.
[10] C. E. Wilmer, M. Leaf, C. Y. Lee, O. K. Farha, B. G. Hauser, J. T. Hupp, R. Q. Snurr, *Nat. Chem.* **2012**, *4*, 83 – 89.
[11] C. E. Wilmer, K. C. Kim, R. Q. Snurr, *J. Phys. Chem. Lett.* **2012**, *3*, 2506 – 2511.
[12] S. S. Y. Chui, S. M. F. Lo, J. P. H. Charmant, A. G. Orpen, I. D. Williams, *Science* **1999**, *283*, 1148 – 1150.
[13] C. E. Wilmer, O. K. Farha, T. Yildirim, I. Eryazici, V. Krungleviciute, A. A. Sarjeant, R. Q. Snurr, J. T. Hupp, *Energy Environ. Sci.* **2013**, *6*, 1158 – 1163.
[14] a) J. B. DeCoste, G. W. Peterson, H. Jasuja, T. G. Glover, Y.-g. Huang, K. S. Walton, *J. Mater. Chem. A* **2013**, *1*, 5642 – 5650; b) J. B. DeCoste, G. W. Peterson, B. J. Schindler, K. L. Killops, M. A. Browe, J. J. Mahle, *J. Mater. Chem. A* **2013**, *1*, 11922.
[15] D. D. Do, *Adsorption Analysis*: *Equilibria and Kinetics*, Imperial College Press, London, **1998**.
[16] L. J. Murray, M. Dinca, J. Yano, S. Chavan, S. Bordiga, C. M. Brown, J. R. Long, *J. Am. Chem. Soc.* **2010**, *132*, 7856 – 7857.
[17] G. W. Peterson, J. B. DeCoste, T. G. Glover, Y. Huang, H. Jasuja, K. S. Walton, *Microporous Mesoporous Mater.* **2013**, *179*, 48 – 53.

